SAND2019-12838C

Designing an Optimized Fixture for the BARC Hardware Using a Parameterized Model

Tyler F. Schoenherr
Sandia National Laboratories[1]
P.O. Box 5800 - MS0346
Albuquerque, NM, 87185

Abstract

Institutions often run dynamic laboratory tests to replicate the environment field stress of a component or system. There are several difficulties in replicating the environment field stress in a laboratory. One difficulty arises if the connection degrees of freedom have relative motion to each other. In that case, the fixturing of the component in a dynamic laboratory test is critical to allow the unit under test to achieve the field displacement and stress. This paper develops and demonstrates a method of producing a test fixture that matches the impedance of the next level of assembly in a way that the component is capable of replicating the dynamic stresses experienced in the field environment. This is done by creating a parameterized model and optimizing it to provide a test fixture for the BARC hardware to satisfy the boundary condition challenge problem.

Keywords
Optimization,Modal Projection Error, boundary condition, fixture, BARC

1 Introduction

Designing a dynamic environment test involves connecting the unit of interest to a driving system by means of a dynamic test fixture. Past design guidelines of dynamic test fixtures are to design them in a way that they have no elastic motion in the frequency range of the test, referred to as a "rigid" fixture. A rigid fixture ensures that the test fixture does not introduce a new natural

[1]Sandia National Laboratories is a multi-mission laboratory managed and operated by National Technology and Engineering Solutions of Sandia, LLC., a wholly owned subsidiary of Honeywell International, Inc., for the U.S. Department of Energy's National Nuclear Security Administration under contract DE- NA-0003525.

frequency as an input to the unit of interest.

By definition, a rigid fixture does not allow for any motion between the connection degrees of freedom of the unit of interest. This is a problem if the field configuration and environment excites the motion of the unit of interest that causes the connection degrees of freedom to move relative to each other. The stress and strain caused by this relative motion cannot be captured in the dynamic environment test.

In order to design a dynamic test fixture, one would like to optimize a fixture so that it most closely resembles the impedance that the unit of interest would see in the field configuration. In order to use an optimization routine, an objective function must be defined. Frequency response functions have been used in the past but have shown empirically that they are prone to several local minima which make the optimization problem difficult or intractable to converge to a meaningful answer. [8]

This paper documents the characterization of several different objective functions' error space. The ability for the objective function to converge to the global minimum is the focus of the characterization. The characterization provides quantifiable results on the robustness of the optimization objective function.

Of the objective functions explored, the Modal Projection Error is used for three separate optimization analyses. One of these analyses includes the Box Assembly with Removable Component (BARC) from the Boundary Condition Challenge Problem.[9] The challenge problem was designed to facilitate research in the design and implementation of a dynamic test fixture in the case that a rigid fixture is an inappropriate choice.

2 Objective Functions

Several objective functions are explored in this study. Most of the objective functions are perturbations of a difference of frequency response function (FRF) objective functions. The differences are between a reference and a trial system. The FRF objective functions are included because they are the easiest to implement in some available softwares.[3][5] FRF based functions have been widely used to limit or minimize the response of a structure at a specific location or the dynamic compliance.[10][4]

The first objective function was the absolute difference between FRFs shown as

$$J_{FRF}(u,\bar{p}) = \sum_{k=1}^{N_{freq}} \left\{ \sum_{m=1}^{N_{loads}} \left(\sum_{i=1}^{N_{dof}} abs(||u_{ikm}|| - ||\tilde{u}_{ikm}||) \right) \right\} \tag{1}$$

where J is the objective function or error, u is the FRF displacements, $\bar{p}$ is the vector of parameters, and the tilde designation over the u variable designates the FRF displacements of the reference system. The variable u is a function of the parameters,$\bar{p}$, but this designation is omitted from the equations in this section for clarity. The objective function in Eqn 1 is chosen because it is a simple method of comparing the FRFs while ignoring phase.

Another objective function examined is the absolute value normalized shown as

$$J_{FRF}(u,\bar{p}) = \sum_{k=1}^{N_{freq}} \left\{ \sum_{m=1}^{N_{loads}} \left(\sum_{i=1}^{N_{dof}} \left[abs\left(\frac{||u_{ikm}|| - ||\tilde{u}_{ikm}||}{||u_{ikm}||} \right) \right] \right) \right\}. \tag{2}$$

Equation 2 is included because it weights all frequencies the same. This is contrary to Eq 1 that biases the difference around the structure resonances due to the relatively large response around the resonances.

Also examined was the difference of the real parts of the FRF shown as

$$J_{FRF}(\bar{u},\bar{p}) = \sum_{k=1}^{N_{freq}} \left\{ \sum_{m=1}^{N_{loads}} \left(\sum_{i=1}^{N_{dof}} abs[real(u_{ikm}) - real(\tilde{u}_{ikm})] \right) \right\} \tag{3}$$

and the imaginary parts of the FRF shown as

$$J_{FRF}(\bar{u},\bar{p}) = \sum_{k=1}^{N_{freq}} \left\{ \sum_{m=1}^{N_{loads}} \left(\sum_{i=1}^{N_{dof}} abs[imag(u_{ikm}) - imag(\tilde{u}_{ikm})] \right) \right\}. \tag{4}$$

The real and imaginary parts were included to see if one part of the FRF was more critical in terms of convergence in the optimization. It was noted that Eq 1 through 4 was not an extensive list of possible FRF to optimize on, but these objective functions provided an overview of their effectiveness to base further decisions of objective function selection.

Another frequency based objective function that was included in this body of research was the Frequency Response Assurance Criteria (FRAC). [2] The FRAC objective function is defined as

$$J_{FRF}(\bar{u},\bar{p}) = 1 - \frac{abs(\bar{u} \cdot \bar{\tilde{u}}^*)^2}{(\bar{u} \cdot \bar{u}^*) \cdot (\bar{\tilde{u}} \cdot \bar{\tilde{u}}^*)} \tag{5}$$

where $\bar{u}$ is now a vector of a concatenation of FRFs in the frequency domain and the superscript * is the Hermitian Transpose. Because a FRAC value converges towards 1 when the frequency response functions equal each other, it is subtracted from 1 so that a low number is desirable and the objective function can be minimized.

The final objective function examined in this paper is based in the modal domain. Gradients of eigenvalues and eigenvectors have been computed in the past [7] with the intent of limiting response and specific locations on the structure. This paper examines the modal projection error (MPE) [8] as the objective function with the intent of matching the dynamics of two structures. The MPE objective function is defined as

$$J(\boldsymbol{\phi}, \mathbf{p}) = \frac{\sum_{n=1}^{m} \left(1 - \bar{\phi}_{Rn}^{+} \boldsymbol{\phi}\boldsymbol{\phi}^{+} \bar{\phi}_{Rn}\right)}{m} \tag{6}$$

where $\boldsymbol{\phi}$ is a finite number of trial mode shapes and $\bar{\phi}_{Rn}$ is the n^{th} mode of a finite set of reference mode shapes, and the superscript $^+$ is the Moore-Penrose pseudoinverse. The MPE is an error

metric that defines the residual of the projection of one set of mode shapes onto another set of mode shapes. The MPE objective function does not consider the natural frequency of the mode shapes, but only how well the mode shapes of the trial system span into each of the reference modes. The mean of those errors was calculated to get the final objective function. The number of modes included in the reference and trial system were important. This is verified in the limit as the error is zero when all modes of the system are included.

3 Characterizing the Error Space

Objective functions in optimizing structures to match dynamics historically have many local minimum [8]. During an optimization calculation, one does not observe the full error space for all of the initial conditions. The study in this section is to calculate the full error space and observe the objective function's behavior with respect to its design parameters.

A one dimension seven degree of freedom system is developed to investigate the differences between the objective functions in Section 2. The system can be found in Figure 1 and it is designed be a system that is simple to model and did not create or eliminate springs elements between degrees of freedom. The values used for the various springs and masses are found in Table 1. Damping is held constant for all of the error space calculations at two percent modal damping for all modes.

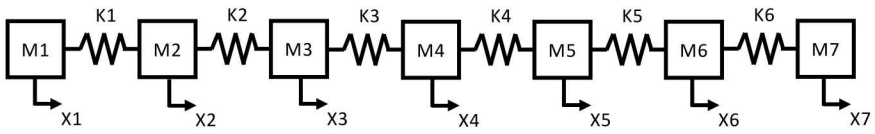

Figure 1: System used to characterize error space of proposed objective functions

Table 1: Dynamic properties of 7 degree of freedom component system

Mass Property	Mass (kg)
M1	5
M2	10
M3	5
M4	7
M5	7
M6	6
M7	6

Stiffness Property	Value (N/m)
K1	1000
K2	800
K3	1100
K4	1000
K5	600
K6	800

3.1 One Design Parameter

The first analysis iteration that examines the error space of the objective functions modifies one design parameter, K2. The design parameter is varied linearly between 10 and 10,000 N/m and the specific FRF that is used in the objective functions is between degrees of freedom 2 and 4. The comparison between frequency response functions objective functions are examined at two different values of frequency spacing, 2 Hz and 0.2 Hz. The objective functions with respect to the design parameter can be found in Figures 2 and 3. Figures 2 and 3 show that all of the frequency based objective functions were not convex throughout the entire design space explored. The error space also showed that the delta frequency parameter plays a key role in these objective functions as a coarse frequency response function will increase the number of local minima. A proper frequency spacing is not established in this study as it is expected that the needed frequency spacing is dependent on the damping of the system

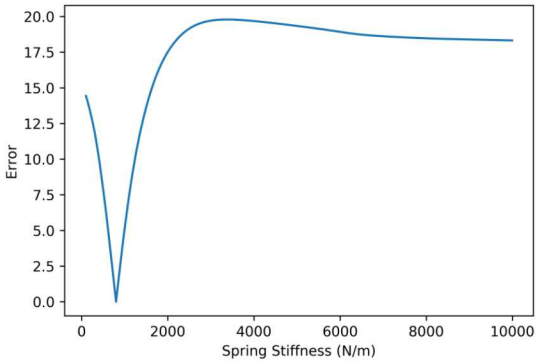

(a) Objective function of FRF absolute value function

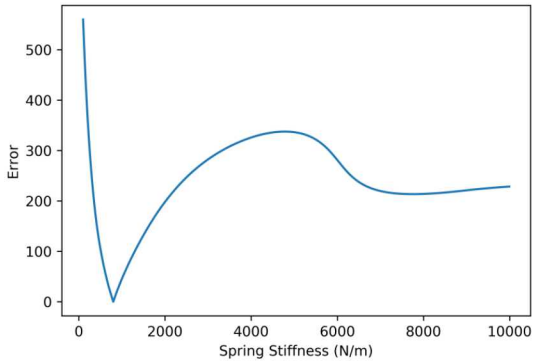

(b) Objective function of normalized FRF absolute value function

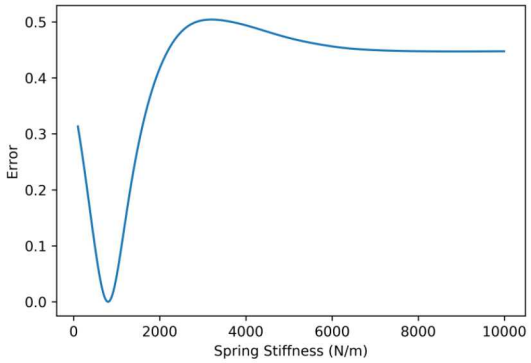

(c) Objective function of FRAC function

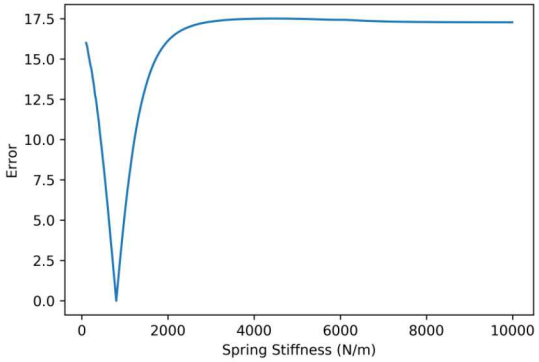

(d) Objective function of FRF real function

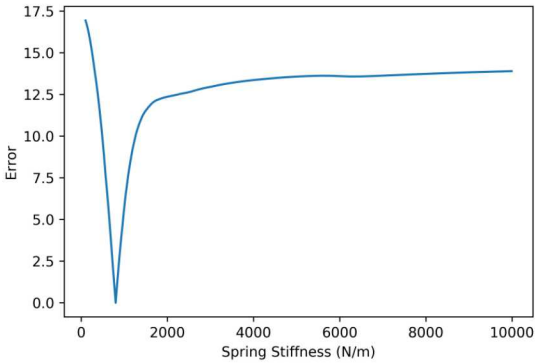

(e) Objective function of FRF imaginary function

Figure 2: Frequency based objective functions and their values with respect to parameter K2 with a frequency spacing of 0.2 Hz

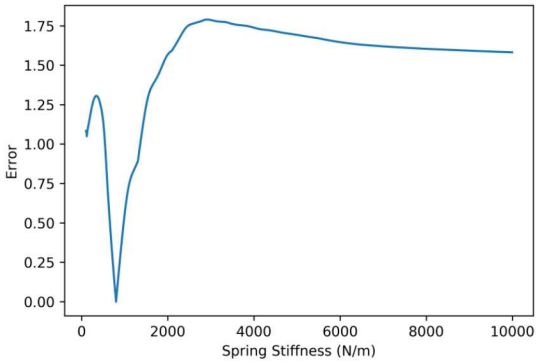

(a) Objective function of FRF absolute value function

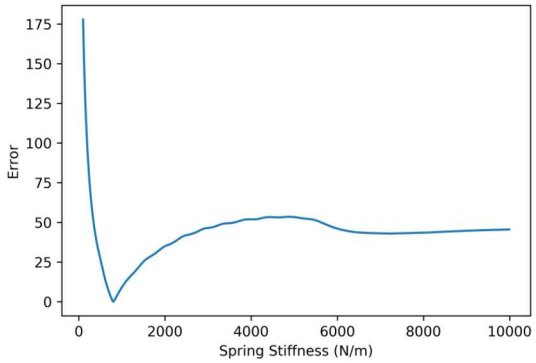

(b) Objective function of normalized FRF absolute value function

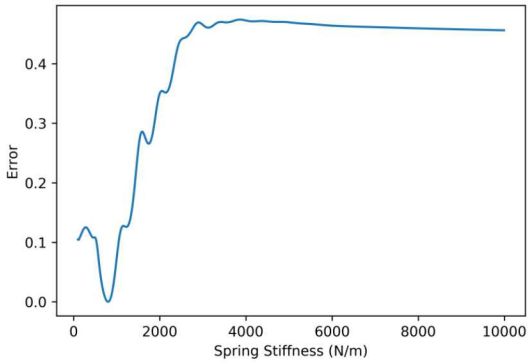

(c) Objective function of FRAC function

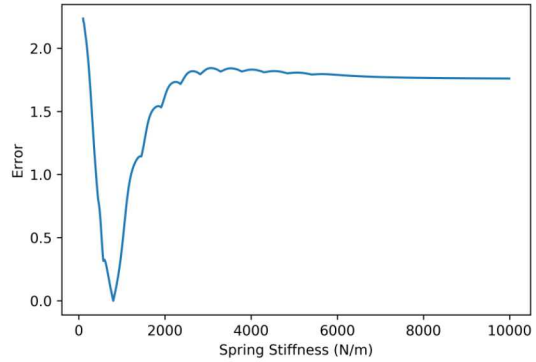

(d) Objective function of FRF real function

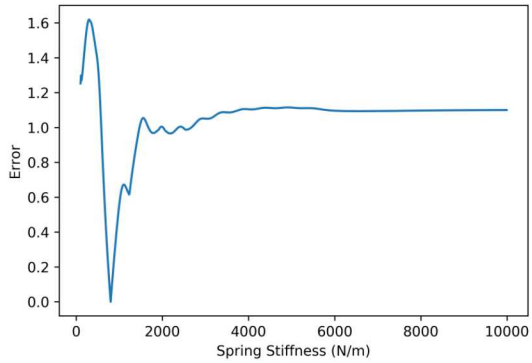

(e) Objective function of FRF imaginary function

Figure 3: Frequency based objective functions and their values with respect to parameter K2 with a frequency spacing of 2 Hz

The error associated with the modal projection error is shown in Figure 4. This objective function does not rely on frequency content, but on how many and which mode shapes are in the objective function. This particular run examined here includes the first two elastic modes of the reference and trial systems. Figure 4 shows that the MPE is convex in the design space explored.

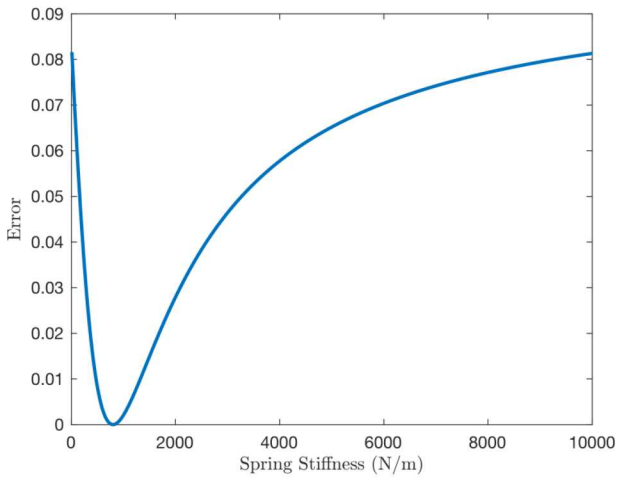

Figure 4: Modal projection error objective function

3.1.1 Two Design Parameters

The next iteration of error space analyses examines the objective functions while varying two design parameters, K2 and K4. The design parameters are varied between 50 and 10,000 Hz, and the FRF used in the objective functions is between degrees of freedom 2 and 4. The observation of the effect on the delta frequency value was noted using two design parameters and the plots were not replicated. The results of the error with respect to the design parameter can be found in Figures 5.

The frequency based errors shown in Figure 5 shows that the error is not convex in the design space explored. It is expected that the amount of local minima would increase as the number of design parameters increased. This was observed in previous attempts to use frequency based objective functions [8]. Three design parameters are considered with respect to exploring the error space. However, the amount of computing needed to fully explore the design space adequately is computationally intractable.

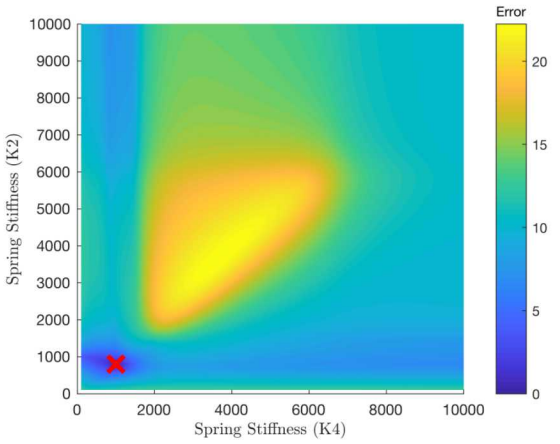

(a) Objective function of FRF absolute value function

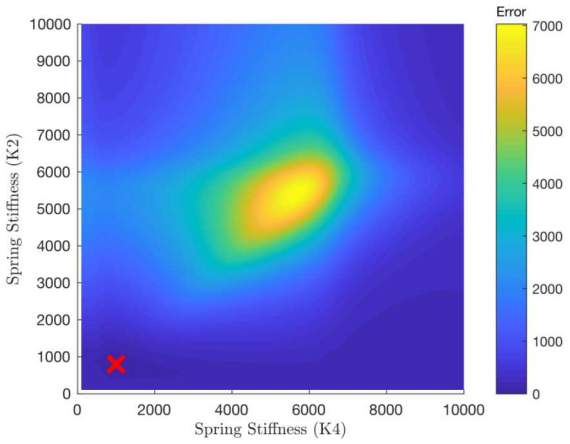

(b) Objective function of normalized FRF absolute value function

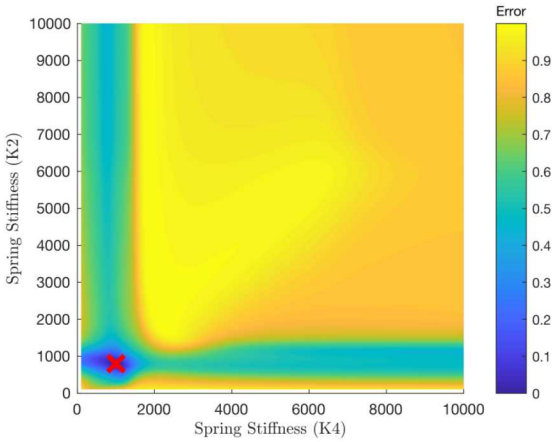

(c) Objective function of FRAC function

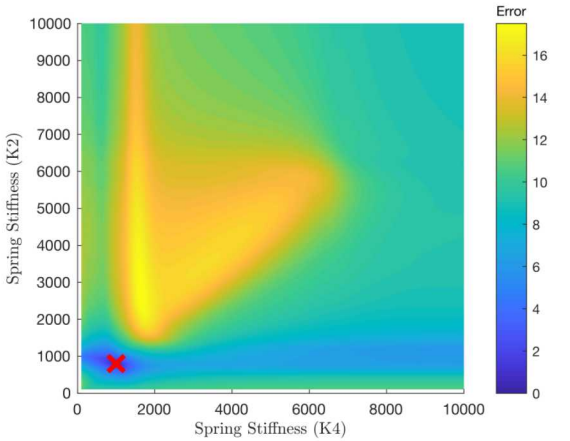

(d) Objective function of FRF real function

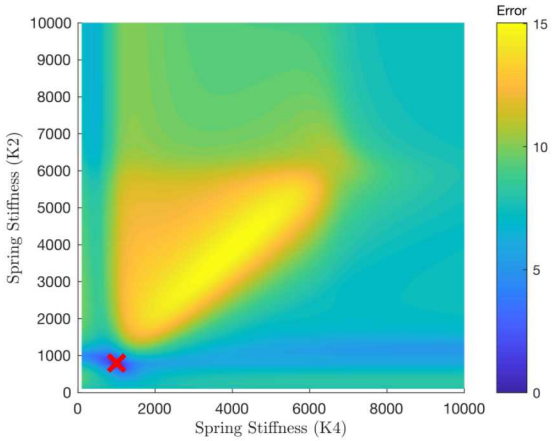

(e) Objective function of FRF imaginary function

Figure 5: Frequency based objective functions and their values with respect to parameter K2 and K4 with a frequency spacing of 0.2 Hz. The 'X' indicates location of global minimum.

The error associated with the modal projection error objective function for two design parameters

is shown in Figure 6. This objective function does not rely on frequency content, but on how many and which mode shapes are in the objective function. This particular run examined here includes the first two elastic modes. Only the modal projection error objective function for two design parameters converged to a single local minima.

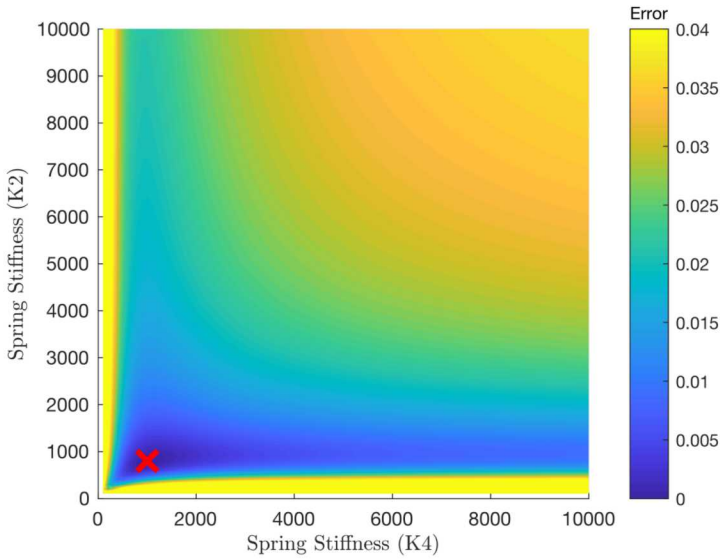

Figure 6: Modal projection error objective function with two design parameters. The 'X' indicates location of global minimum.

Increasing the number of design parameters or increasing the design space is expected to increase the number of local minima for the frequency based objective functions. It is also expected that the topology of the error space for these objective functions will change as the system changes from a seven degree of freedom system to a more complex one. Computing the complete error space for three or more design parameters without restricting the design space becomes intractable even for a simple system due to the number of combinations of design parameters. The remainder of this paper investigates optimization analyses as the method of designing impedance matched structures. The MPE objective function is used on several systems to explore convergence to a global minima and the prospect of using optimization with MPE .

4 Optimizing Impedance Matched Structures

This section presents the execution of optimization analyses using MPE as the objective function for different case studies. These case studies are on a variety of different dynamic systems with varying levels of complexity. The systems are a seven degree of freedom system introduced in Section 3, a three dimension double beam structure, and the Box Assembly with Removable Component (BARC) structure which is designed to challenge the creation of impedance matched structure. [**?**] These runs systematically investigate aspects of the optimization problem with respect to parameters to the MPE objective function and the setting of the initial conditions.

All of the optimization runs in this section utilize the `FMINCON` optimization algorithm developed by Matlab [6]. Since analytical derivatives are not available, the finite difference method is used. No work is done to investigate the effectiveness of alternate optimization algorithms to improve results or reduce the number of iterations. The purpose of this paper is to investigate the effectiveness of the objective function with respect to developing an impedance matched structure.

4.1 Case Study 1 of Impedance Matching

The system shown in Figure 1 is used for the first optimization analysis. Five parameters are chosen as the design parameters. The five design parameters are five spring constants, K1 through K5, shown in Table 1.

Although the full error space is not calculated on the 5 parameter system due to the number of possible combinations, a random sample of the error space is acquired to get a sample of the error space to determine how convex it is. This random sampling is done by allowing the initial condition of each of the parameter springs to be a random number between 20 and 30,000 N/m. Ten thousand iterations of the optimization analysis is computed and the number of occurrences that resulted in a solution that isn't the global minimum is tracked. The global minimum is defined to be when the design parameters matched the stiffness values within given in Table 1 to a tolerance of 0.1%.

Through exploration of the objective function, it is discovered that the number of modes included in the MPE calculation has an effect on the error space of the objective function. The number of modes included is varied and the number of optimization solutions that failed to converge to the reference values are tracked and listed in Table 2 with each study having an unique set of initial conditions. In this case study, it is found that more modes included in the objective function made the problem more convex, however, future case studies found that simply adding more modes did not provide a more convex problem. The content of the modes in relation to each other appears to be important. This is shown by comparing the number of failures using modes one through three and two through three. Using only modes two through three provided a more convex error space.

Table 2: Count of the local minima in the design space of a five parameter optimization analysis for a seven degree of freedom system (10,000 attempts)

Modes Included in the MPE Objective Function	Count of Failed Attempts to Converge to the Global Minimum
Modes 1 through 4	2
Modes 1 through 3	2007
Modes 1 through 2	5231
Modes 2 through 3	577

Table 2 did not fully describe the convex nature of the error space in the optimization problem. It is discovered that the optimization algorithm played a part in the optimization not converging to the global minimum. Both the failed runs for the MPE objective function that uses modes one through four converges when restarted from the final converged parameters.

Some of failed runs when modes one through three are used in the MPE calculation are examined. Of the sampled failed runs, a line is drawn between the respective last iteration and the global minimum with respect to the five parameters. Examination of this line showed if the final iteration is truly a local minima or if there existed a direction the optimizer could take to reduce the error. All of the runs that failed to converge to the global minimum when modes one through three are used are not local minima. This indicates that the optimizer algorithm failed to find the correct gradient to reduce the objective function. However, some solutions when only modes one and two are used are a local minimum when examining the error space between the final iteration and global minimums.

Also examined is the convergence of the objective function and how many iterations are needed to converge. Figure 7 shows an example of an objective function curve for the MPE objective function. Figure 7 shows that there are long periods where the iterations do very little to change the error of the objective function which implies that the gradients of the objective function are very small in some locations or that the optimization algorithm is poor at identifying the correct direction for minimizing the objective function. More research can be done to determine if different algorithms would behave better and provide a better solution in fewer iterations. The iterations in Figure 7 do not include the analysis runs that were used to determine the derivatives using the finite difference method.

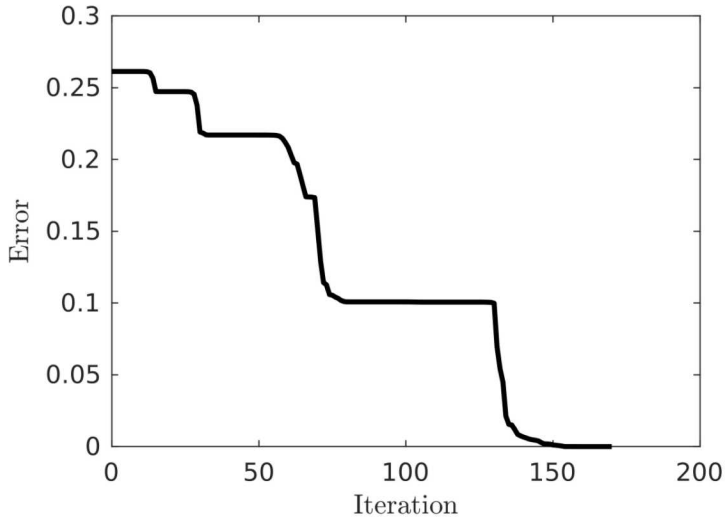

Figure 7: A sample convergance curve for the seven degree of freedom system using Matlab's [6] `FMINCON`

4.2 Case Study 2 of Impedance Matching

The second case study includes a three dimension finite element model with fifty thousand degrees of freedom. This system is shown in Figure 8. This system is designed to modify the posts and bottom beam to match the modes of the top beam in the reference system. The five design parameters in this optimization analysis are the dimensions of the posts and bottom beam and they are labeled in Figure 8. These parameters are perturbed to see if they can converge back to the original

dimensions. The degrees of freedom included in the MPE calculation are the degrees of freedom of the nodes associated with the top or yellow component beam in Figure 8. The other degrees of freedom are not included in the MPE calculation because the optimization is designed to match the response of the component only and not the system to which it is attached.

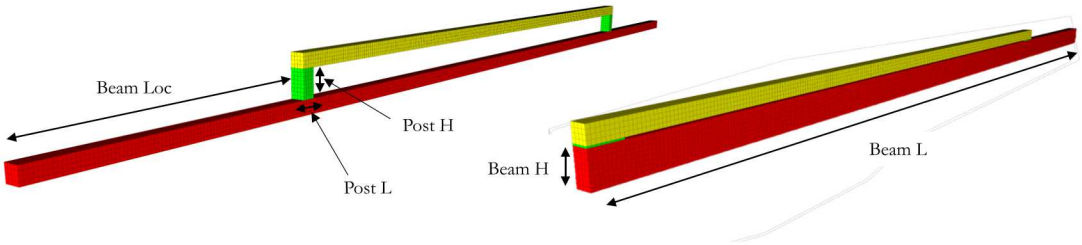

Figure 8: Three dimension beam system with a component beam (yellow), posts (green), and support beam(red). Design parameters are labeled. The reference system (left) and initial condition (right) are shown.

Initial conditions are chosen to make the initial condition system to have higher natural frequencies than the reference system and the optimization run to match the first three elastic modes. The optimization consistently converges to the global minimum if the initial conditions of the parameters are set in a way that results in the trial structure having higher natural frequencies than the reference system. This is an expected observation as the modal projection error is more efficient if the trial modes are independent of each other. If the fixture or support structure is soft, there are modes of the component or yellow beam that repeat as the modes only change in the support structure. The initial condition, the reference solution, and the optimized solution can all be found in Table 3. The structure with the initial condition values can be seen in Figure 8. Starting with a rigid initial condition and a small set of modes consistently produces the global minimum.

Table 3: Initial, Final and Reference values for the five parameter double beam case study

	Reference	Initial	Optimized
Beam L	100 in	80 in	100.01 in
Beam H	1.00 in	2.0 in	1.0033 in
Beam Loc	20.0 in	0.0 in	20.000 in
Post W	2.00 in	0.1 in	2.0034 in
Post H	1.00 in	2.0 in	0.9992 in

4.3 Case Study 3 of Impedance Matching

The third case study is on a structure designed to challenge the creation of a impedance matching test structure, dubbed the BARC (Box Assembly with Removable Component). [9] The purpose of the BARC structure shown in Figure 9 is to replace the box assembly that has a slot with an alternative structure that provides the same dynamics as the box assembly with the component. This structure is difficult to replace because the dynamics of the component and the box assembly are coupled as shown through the first two elastic mode shapes in Figure 10.

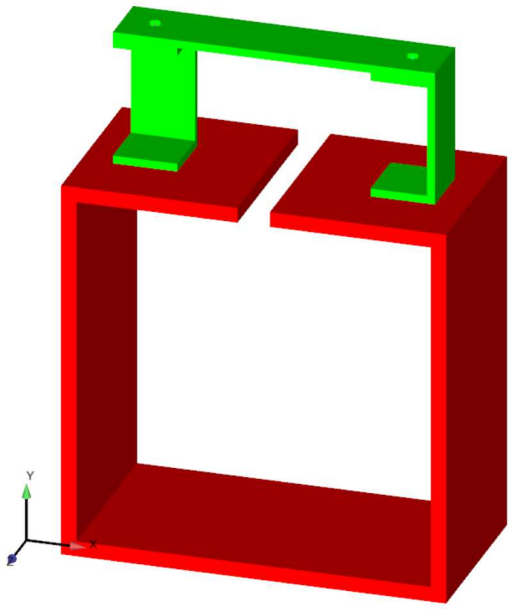

Figure 9: BARC Hardware with the Box Assembly (red) and Removable Component (green)

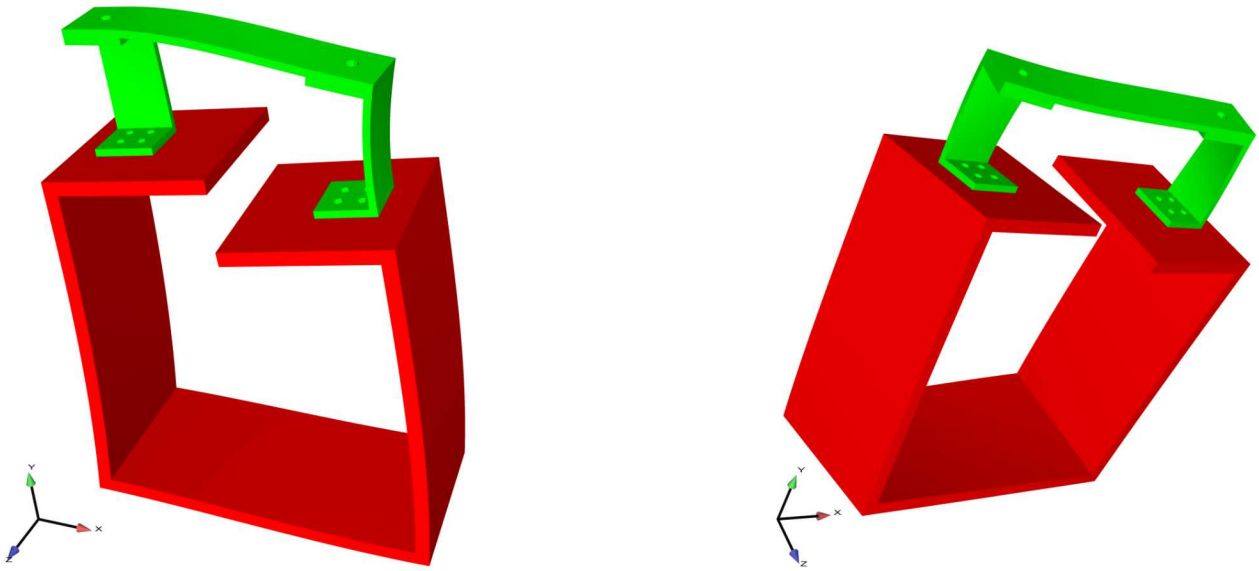

(a) 1st elastic mode (b) 2nd elastic mode

Figure 10: First two elastic modes of the BARC structure

The BARC hardware is parameterized and nodes from the Removable Component are selected for the MPE objective function. The parameterized model and the nodes selected for the MPE calculation can shown in Figure 11.

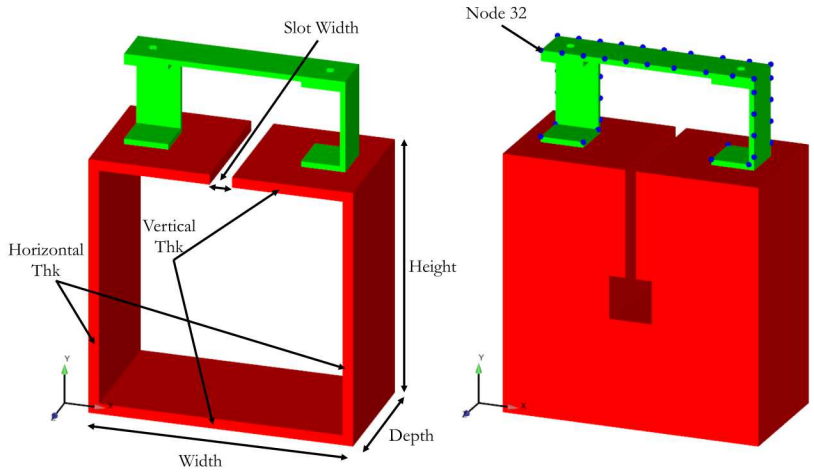

Figure 11: Parameterized BARC Hardware (left) and the optimization initial condition with nodes indicated by blue dots for MPE calculation (right)

The first eight elastic modes from the reference and trial solutions are used in the MPE calculation for the optimization. The natural frequencies of the first eight elastic modes of the reference system are between 185 and 670 Hz. The initial, reference, and resulting parameters can be seen in Table 4.

Table 4: Initial, Final and Reference values for the BARC case study

	Reference	Initial	Optimized
Horizontal Thickness	0.238 in	2.25 in	0.230 in
Vertical Thickness	0.238 in	2.25 in	0.237 in
Slot Width	0.5 in	0.25 in	0.634 in
Height	6 in	6 in	5.896 in
Width	6 in	6 in	5.97 in
Depth	3 in	3 in	3.1 in

The optimized values do not exactly match the reference values as well as the first two case studies. The slot width parameter is the poorest match. The slot width parameter is the worst match as that parameter has little effect on the dynamics of the removable component when the vertical thickness parameter became small. The slot width only modifies the mass slightly and does nothing to change the stiffness.

To determine how close the dynamics are between the optimized structure and the reference structure, a plot of the driving point frequency response function for node 32 designated in Figure 11 is computed and plotted for both systems in Figure 12. It is determined that the optimization solution produced a structure with a similar impedance to the box assembly.

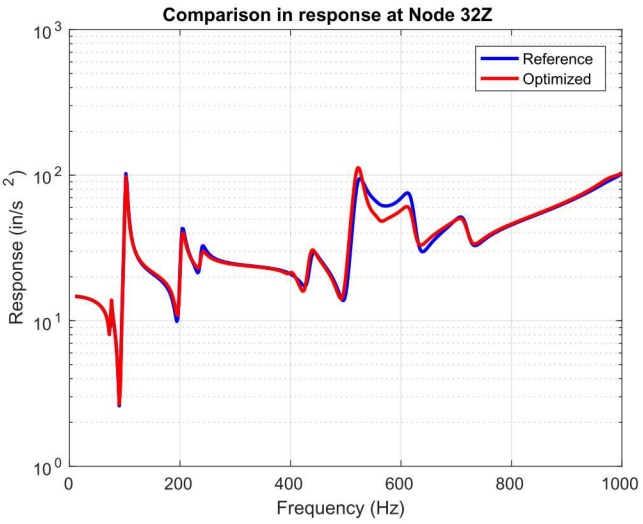

Figure 12: Comparison of driving point frequency response functions at node 32 for the reference and optimized BARC system

4.4 Developing a Non-Trivial Impedance Matched Structure

The case studies in sections 4.1 through 4.3 are designed to determine the effectiveness and ability of the MPE as an objective function for matching the dynamics. These examples are effective because the design space included the global minimum to which the optimization analysis could converge.

These case studies show that the MPE as an objective function is effective in obtaining the goal of modifying our geometry to match dynamic impedance for a specific component.

The next question is how the optimization analysis works if the global minimum is not in the design space of the optimization analysis and if an intermediate solution provides an acceptable structure. This is explored by augmenting constraints for the BARC optimization analysis in Section 4.3. The parameters of the model are unchanged from Section 4.3, but the height parameter is constrained to be below four inches.

The parameters chosen for the initial conditions are selected for the optimization analysis and are in Table 5. The system with the initial conditions can be seen in Figure 13. The MPE objective function includes the first eight elastic modes of the system. The solution for this optimization analysis is computed and then the result is restarted as the initial condition where the first two elastic modes are used in the objective function. The result of the final optimization function can be seen in Figure 14 and Table 5.

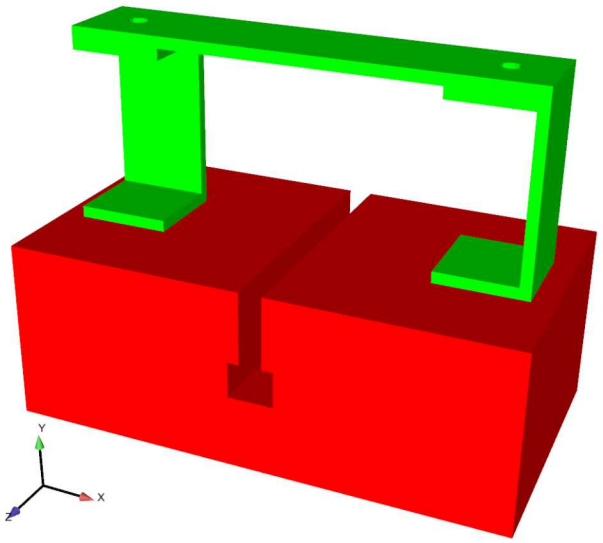

Figure 13: Initial condition for the BARC optimization analysis with height constrained to four inches

Table 5: Initial, final and reference values for the constrained BARC case study

	Reference	Initial	Optimized
Horizontal Thickness	0.238 in	2.5 in	0.18 in
Vertical Thickness	0.238 in	2.5 in	0.23 in
Slot Width	0.5 in	0.25 in	0.41 in
Height	6 in	3 in	3.98 in
Width	6 in	6 in	7.05 in
Depth	3 in	3 in	3.9 in

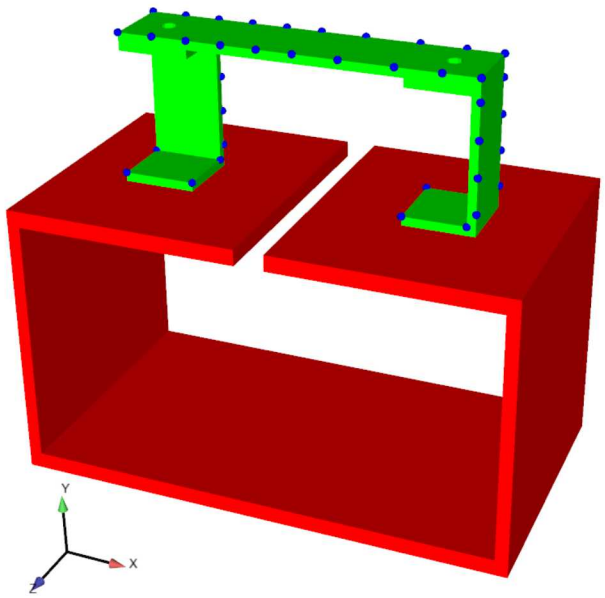

Figure 14: Optimization result of the BARC optimization analysis with height constrained to four inches

Because the global minimum does not exist in the design space for the constrained optimization analysis, a method of determining success is developed. The purpose of using optimization in this paper is to design a test fixture that allows the response of the component in a test fixture to match the response of the component in its field or reference system. If the motion response over the entire structure matches, the stress would also match.

To provide comparison and contrast to the optimally designed test fixture, the component on a rigid test fixture is also analyzed. The rigid fixture used is the initial condition for the optimization with height constraint as shown in Figure 13. It is determined that this fixture is rigid in the bandwidth of interest because the first mode where the fixture exhibited elastic motion is at 2660 Hz.

To obtain a target, or field, stress environment, a forcing function of amplitude 1 lb over frequencies 10-1000 Hz is applied on the reference system at node 32 in the Z direction shown in Figure 11. This environment creates a target stress distribution in the removable component and corresponding motion response.

To try and replicate the field environment, three forces are placed on the rigid and optimized fixture systems. The locations of the three forces are chosen to be at points with high modal displacement in the reference solution and can be seen in Figure 15. Although three independent forces are prescribed in a finite element model, these forces could be applied to a physical structure as has been done previously through techniques such as IMMAT. [1] The input forces are derived to provide a least squares fit to match the response of the nodes indicated in Figure 14.

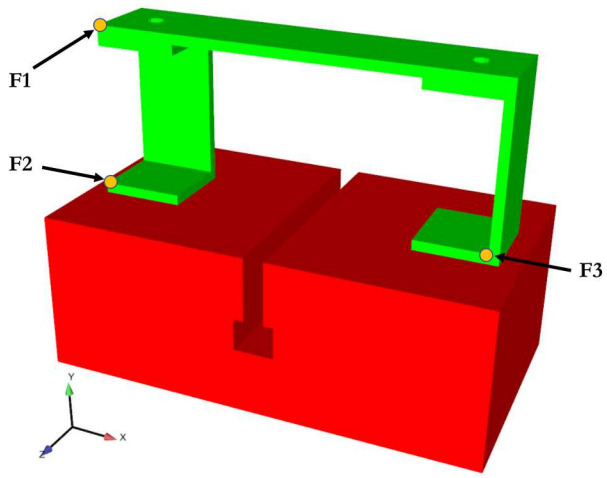

Figure 15: Location of forces on the removable component attached to a rigid fixture

The calculated forces are applied to the component attached to the rigid and optimized fixtures. The response at node 32 for both systems is measured and plotted in Figure 16. From the acceleration comparison, it appears that the optimized fixture is slightly better. Although acceleration response is a typical method of comparing dynamic environments, it is determined that the stress field is a global response and the quantity of interest.

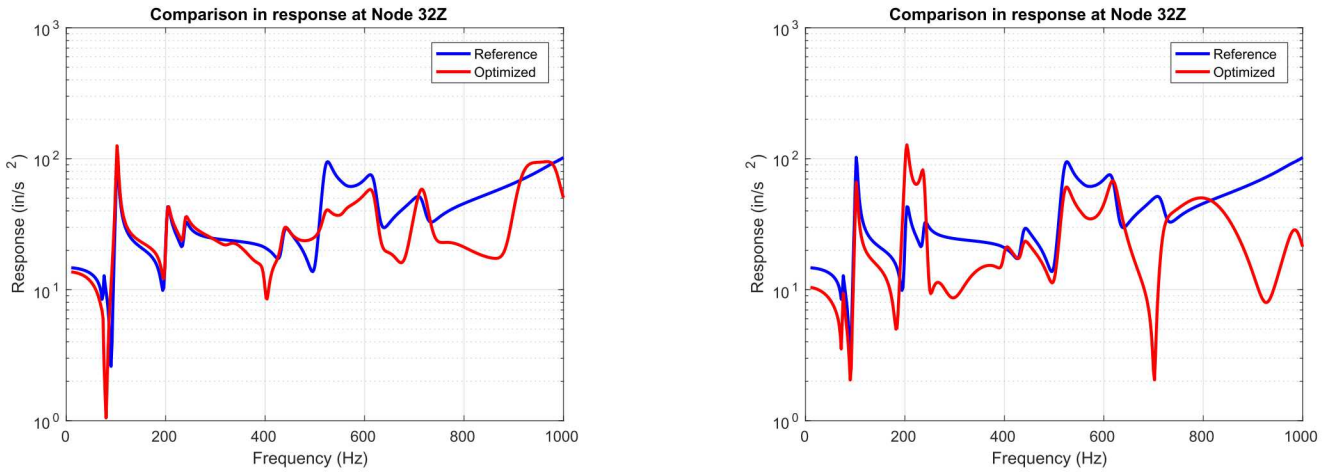

(a) Optimized fixture

(b) Rigid fixture

Figure 16: Response of node 32 from forces imparted on two systems attempting to replicate a reference environment

The root mean squared value of Von Mises stress is calculated over the excitation frequency bandwidth. The comparison between the reference, rigid fixture, and optimized fixture can be

seen in Figure 17. Figure 17 qualitatively shows the improvement made by the optimized test fixture as the stress values for the rigid fixture are a significant over-test in some sections of the removable component.

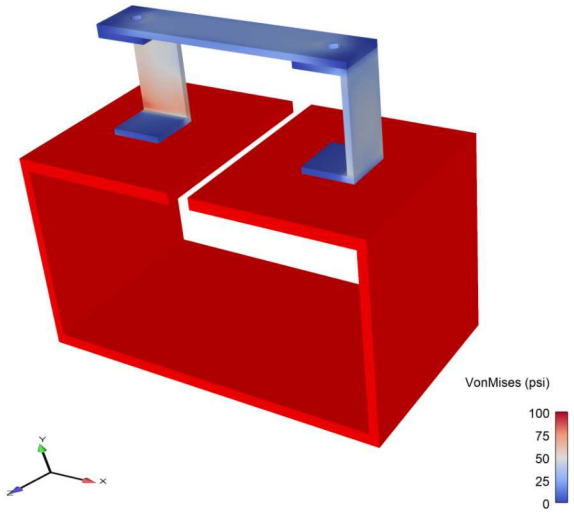

(a) Optimized fixture

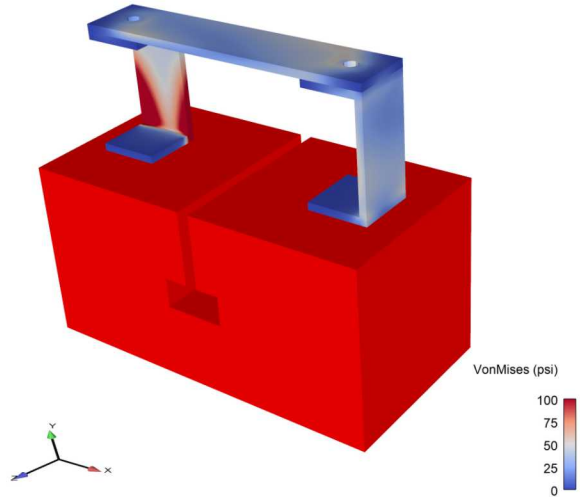

(b) Rigid fixture

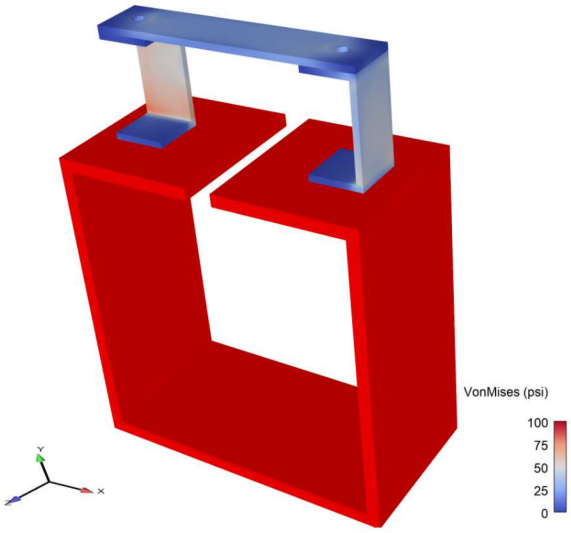

(c) Reference BARC structure

Figure 17: Root mean squared quantities of Von Mises stress of the removable component for the hypothetical environment

The root mean squared stress for the removable component with the optimized test fixture is much closer to the reference system environment when compared to the rigid fixture as shown in Figure 17. However, the root mean squared stress typically is focused on one or two modes at low frequencies. A couple of elements of interest are selected and their stress quantities calculated over the entire

bandwidth. The elements of interest are selected to be areas of higher stress and can be seen in Figure 18.

The stress comparison at these element locations can be found in Figure 19 and 20. Figures 19 and 20 show that the optimized test fixture provides a closer stress response to the reference environment than the rigid fixture over the entire bandwidth. It is the difference in the mode shapes at the natural frequencies that cause the errors in stress at the given locations. For this example and environment, most of the elements in the removable component when connected to the rigid fixture have higher stresses than the reference environment. However, there are locations and modes where the stress is lower than the reference, which disputes the assumption that a rigid fixture is conservative with respect to stress and acceleration.

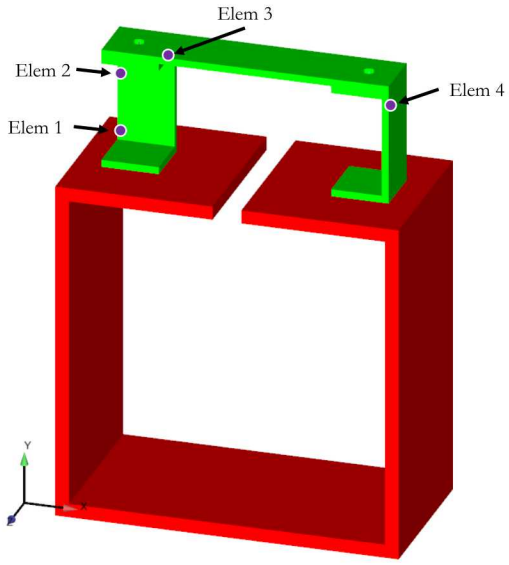

Figure 18: Location of elements used for stress comparison in the frequency domain

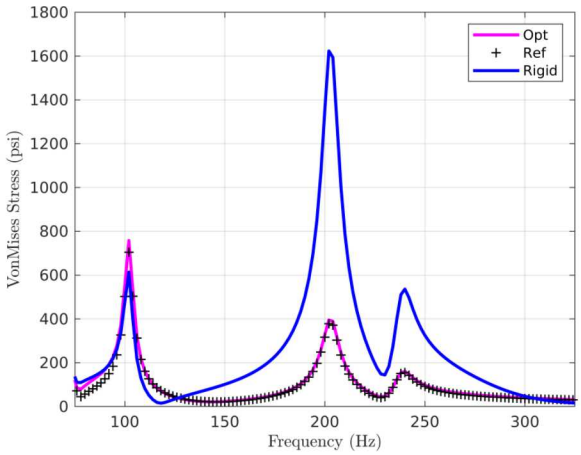

(a) Element 1

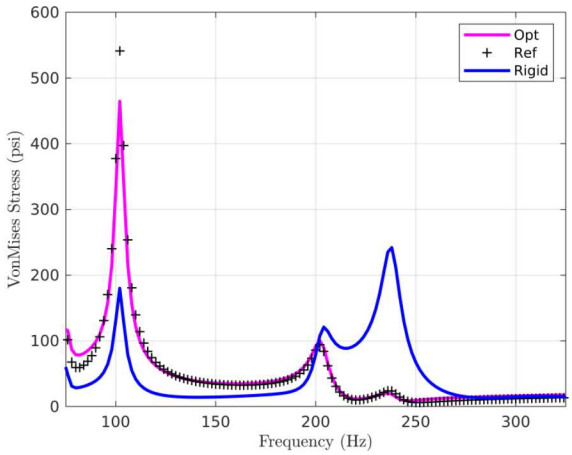

(b) Element 2

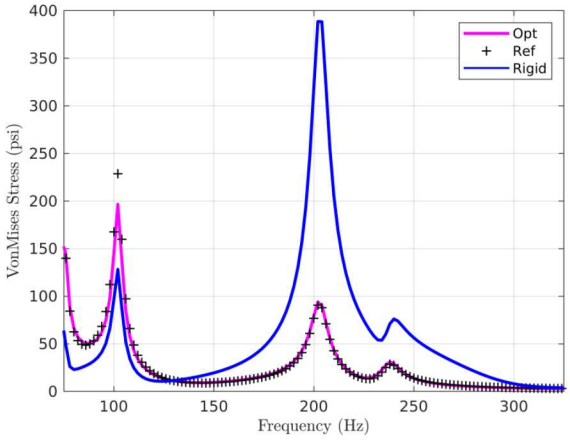

(c) Element 3

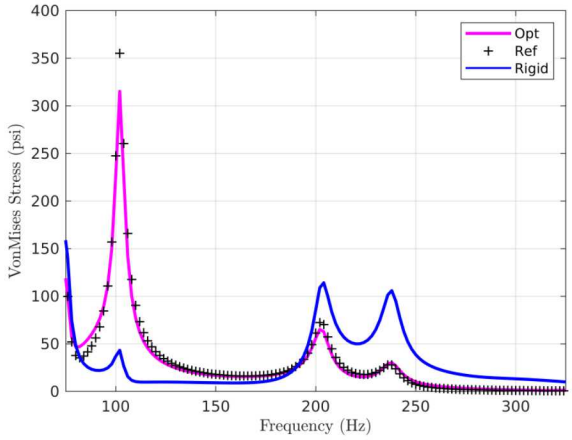

(d) Element 4

Figure 19: Von Mises stress plots of specific removable component elements for the hypothetical environment at low frequencies

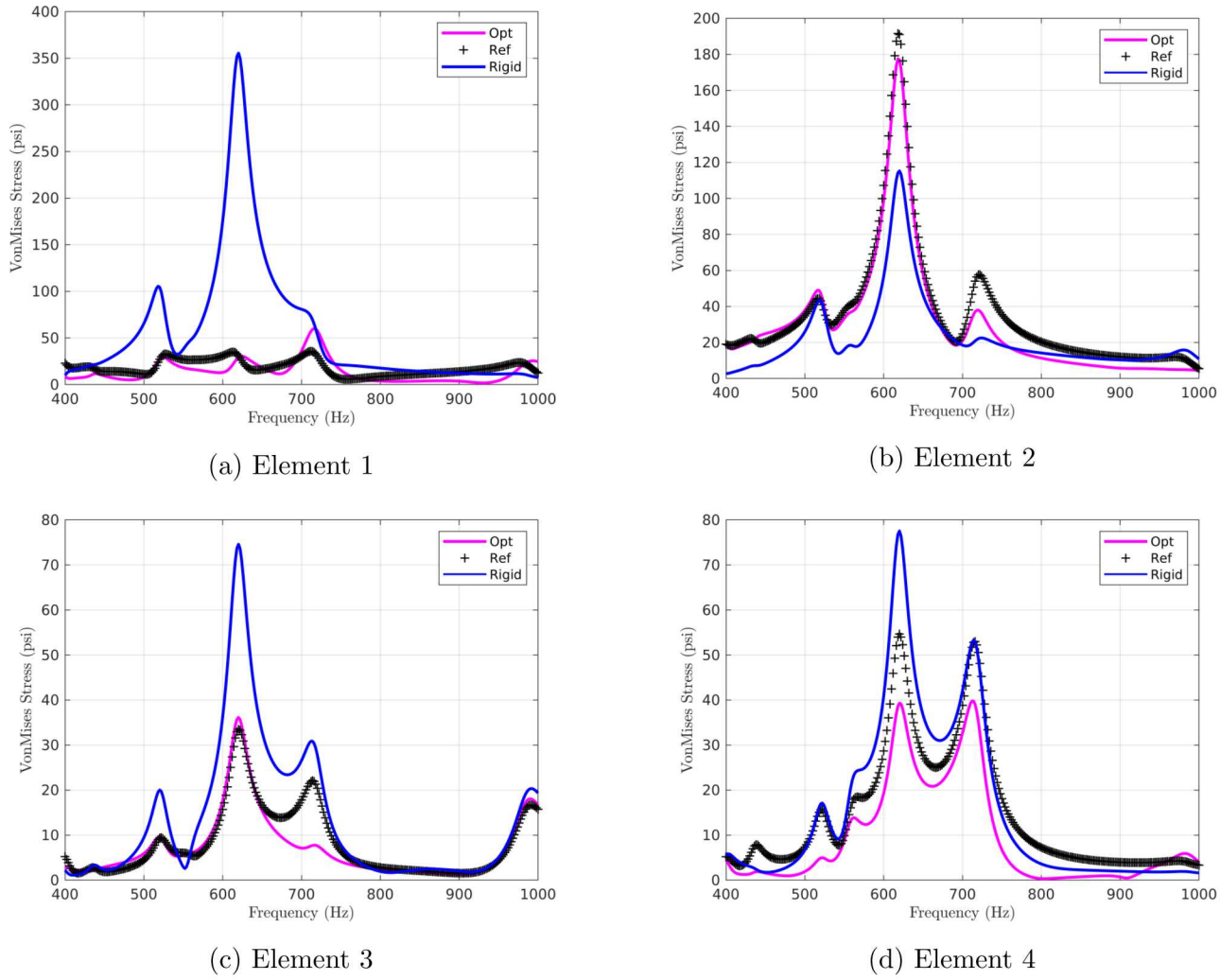

(a) Element 1

(b) Element 2

(c) Element 3

(d) Element 4

Figure 20: Von Mises stress plots of specific removable component elements for the hypothetical environment at high frequencies

5 Conclusion

The purpose of the research presented in this paper is to investigate and characterize objective functions with the intent of designing a test fixture that would represent the impedance of another structure using optimization analysis. A group of objective functions are introduced and the error space is characterized for a set of parameter limits. From this characterization, the MPE is determined to be the best objective function for converging to a desired result. This is because the MPE objective function is shown to be convex for a simple system that had two design parameters while the other objective functions are not convex.

Although the MPE objective function is shown to be convex for a two parameter optimization, the result is dependent on how many and which modes are included in the calculation. There are cases in even the two parameter optimization where the solution does not converge when not enough modes are used in the objective function. Non-converging solutions are also observed for the one

dimension system with five design parameters when not enough modes are used.

The MPE is used as the objective function for three optimization analyses. These analyses show that the number of modes included in the optimization had an effect on the convergence to the global minimum. Although the relationship between what modes to include and the convex nature of the optimization space isn't established, it is found that there existed a combination of modes that did provide an error space that is convex and the result converges to the global minimum.

The optimization algorithm is Matlab's `FMINCON`. No work is done to show that these algorithms provide the best or most efficient methods for optimizing the test fixture. However, evidence shows the algorithms struggle to find the direction of negative gradient as is found from the first case study when the problem is restarted from the previous converged state and the problem then converges to the global minimum.

A non-trivial fixture is created to replace the box assembly for the BARC structure. The fixture is non-trivial because the optimized structure is not allowed to converge to the reference structure. This is significant because it shows that there can exist a solution structure that represents the dynamics of the reference structure. The solution is shown to be an improvement through examination of a mock field environment where the stresses are measured.

References

[1] P. M. Daborn, C. Roberts, D. J. Ewins, and P. R. Ind. *Next-Generation Random Vibration Tests*, pages 397–410. Springer International Publishing, Cham, 2014.

[2] Ward Heylen, Stefan Lammens, Paul Sas, et al. *Modal analysis theory and testing*, volume 200. Katholieke Universiteit Leuven Leuven, Belgium, 1997.

[3] Hyperworks. Optistruct, 2018.

[4] J.S. Jensen. Topology optimization of dynamics problems with padé approximants. *International journal for numerical methods in engineering*, 72(13):1605–1630, 2007.

[5] Sandia National Laboratories. Plato, 2018.

[6] Mathworks. Matlab r2019a, 2019.

[7] J.H. Rong, Y.M. Xie, X.Y. Yang, and Q.Q. Liang. Topology optimization of structures under dynamic response constraints. *Journal of Sound and Vibration*, 234(2):177–189, 2000.

[8] T. Schoenherr, B. Clark, and P. Coffin. Improve replication of in-service mechanical environments. Technical Report SAND2018-10187, Sandia National Laboratories, September 2018.

[9] David E. Soine, Richard J. Jones, Julie M. Harvie, Troy J. Skousen, and Tyler F. Schoenherr. Designing hardware for the boundary condition round robin challenge. In *Topics in Modal Analysis & Testing, Volume 9*, pages 119–126, Cham, 2019. Springer International Publishing.

[10] G.H. Yoon. Structural topology optimization for frequency response problem using model reduction schemes. *Computer Methods in Applied Mechanics and Engineering*, 199(25-28):1744–1763, 2010.

Distribution:

Schoenherr T., Org 1553